



<Research Article>

Development of a 2-oxobutyrate dehydrogenase through structure-based enzyme design and its application in a 2-oxobutyrate assay

Momoka Nakamura¹ and Yoshiaki Nishiya^{1,2,*}

Summary Based on the structure-guided computational design of *Geobacillus stearothermophilus* lactate dehydrogenase (gs-LDH), we have already succeeded in developing a phenylpyruvate-specific dehydrogenase. As a new subject, a 2-oxobutyrate (2OBA)-specific dehydrogenase was developed through structure-based enzyme design of gs-LDH. *In silico* analysis of gs-LDH identified a Q-to-V mutation at position 102, considering the substrate-binding site in accordance with the 2OBA structure and its interactions with the methyl group. However, the improvement in 2OBA specificity of Q102V was insufficient. Therefore, an additional mutation A248L, whose energetic destabilization of pyruvate (the native substrate) binding was revealed by docking analysis of gs-LDH, was introduced. The 2OBA/pyruvate activity ratio of the Q102V+A248L double mutant was 620%, compared with 57% for the wild-type gs-LDH. Thus, a 2OBA-specific dehydrogenase was successfully developed. A 2OBA endpoint assay reagent containing the double mutant was prepared, and its practicality was preliminarily confirmed.

Key words: 2-Oxobutyrate, Lactate dehydrogenase, Tertiary structure, Mutagenesis, Computational design

1. Introduction

Lactate dehydrogenase (LDH, EC 1.1.1.27) and malate dehydrogenase (MDH, EC 1.1.1.37) are used to analyze biological samples¹⁻³. LDH is used to measure alanine aminotransferase, lactate, and ADP (with pyruvate kinase). By contrast, MDH is used to measure aspartate aminotransferase, malate, bicarbonate (with phosphoenolpyruvate carboxylase), and citrate (with citrate lyase). Despite their functional and structural similarities, LDH and MDH differ in

their substrate specificity^{3,4}. We succeeded in elucidating the detailed mechanism of the structural changes leading to both enzyme reactions and explaining the high substrate specificity of MDH⁴⁻⁷. Furthermore, structural and molecular dynamics analyses provided an understanding of the differences in substrate specificity between LDH and MDH⁴.

The results highlight the importance of three elements: (1) the charge of the active site in the apoenzyme, (2) movement of the catalytic histidine residue, and (3) flexibility of the mobile loop in the

¹Division of Life Science, Graduate School of Science and Engineering, Setsunan University, 17-8 Ikeda-Nakamachi, Neyagawa, Osaka 572-8508, Japan.

²Department of Life Science, Setsunan University, 17-8 Ikeda-Nakamachi, Neyagawa, Osaka 572-8508, Japan.

*Corresponding author: Yoshiaki Nishiya, Department of Life Science, Setsunan University, 17-8 Ikeda-Nakamachi, Neyagawa, Osaka 572-8508, Japan.

Tel: +81-72-800-1151

Fax: +81-72-838-6599

E-mail: nishiya@lif.setsunan.ac.jp

Received for Publication: October 2, 2025

Accepted for Publication: December 1, 2025

active site during structural changes. The combined effect of these three elements provides a strategy for MDH to achieve high substrate specificity. However, the simple reaction mechanism of LDH is unaffected by these elements, resulting in reduced substrate selectivity^{8,9}. Thus, LDH is a desirable basis for functional alteration of substrate specificity because of its relatively simple dynamic response^{1,2,10-12}. A structural understanding of substrate specificity provides a theoretical basis for structure-based computational design for the development of diagnostic enzymes¹³.

Using structure-based enzyme design, we have already succeeded in altering the substrate specificity of LDH and developing a phenylpyruvate (PPY)-specific dehydrogenase¹⁴. In the present study, a 2-oxobutyrate (2OBA)-specific dehydrogenase was developed using a structure-based design. LDH from *Geobacillus stearothermophilus* (gs-LDH)^{1,2} was used as the basis for site-directed mutagenesis, as described in a previous study on PPY dehydrogenase. Similar to PPY, 2OBA is a minor substrate of LDH and is structurally similar to the major and native substrate, pyruvate (PYR) (Fig. 1). Since the high similarity of 2OBA to PYR reduces the likelihood of identifying effective mutations, the construction of a 2OBA-specific enzyme based on rational design is more difficult than that of a PPY-specific enzyme.

2OBA is an intermediate in methionine metabolism and is synthesized from cystathionine, along with cysteine. Disorders in methionine metabolism cause the accumulation of homocysteine and its dimers (homocystine), resulting in homocystinuria, which is associated with disorders of the nervous, skeletal, and vascular systems^{15,16}. We believe that the simple and rapid enzymatic measurement of

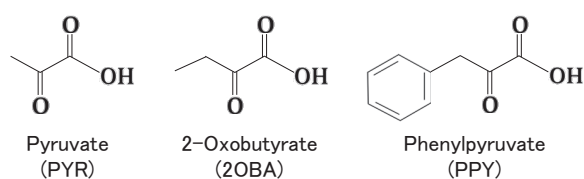


Fig. 1. Substrate structure of *Geobacillus stearothermophilus* lactate dehydrogenase (gs-LDH).

2OBA is of clinical significance. Thus, a 2OBA endpoint assay reagent containing the developed enzyme was prepared, and its practicality was preliminarily confirmed.

2. Materials and Methods

Computational analysis

Based on the gs-LDH tertiary structure (PDB ID: 1LDN)¹, *in silico* analysis and rational mutation design were performed using the Molecular Operating Environment software (MOE, Chemical Computing Group Inc., Montreal, Canada)^{17,18}. Before energy minimization, the force field Amber10:EHT was used to add hydrogen atoms and partial charges according to the manufacturer's instructions. Relaxation of the added hydrogen atoms via energy minimization was performed using a conjugated gradient/truncated Newton optimization algorithm with a convergence criterion of 0.05 kcal/mol. Complex structural models of the wild-type (WT) and mutant enzymes containing 2OBA or PYR were constructed using docking simulations according to the manufacturer's instructions. The molecular structures of the compounds used in the docking simulations were obtained from PubChem (<https://pubchem.ncbi.nlm.nih.gov/>). The enzyme structure and 2D-depict models were visualized using the MOE software.

Reagents and chemicals

All reagents and chemicals were purchased from Nacalai Tesque, Inc. (Kyoto, Japan) and Wako Pure Chemical Industries, Ltd. (Osaka, Japan).

Site-directed mutagenesis

The expression plasmid for gs-LDH was used to prepare the WT and served as a template for site-directed mutagenesis, as previously described¹⁴. The plasmid encodes gs-LDH (317 amino acid residues) and 20 additional amino-terminal residues containing a six-histidine tag. Expression plasmids for the mutants were prepared by inverse polymerase chain reaction using KOD-plus polymerase (Toyobo Co., Ltd., Osaka, Japan) according to the manufacturer's

Table 1 Specific PCR primers used for site-directed mutagenesis

Q102A	Forward	5'- <u>GTG</u> AAACCGGGTAAACCCGTCTGGACCT-3'
	Reverse	5'-GTTTCGCACCCGCGCAAATCACAACCAGAT-3'
A248L	Forward	5'- <u>CTG</u> ACCTACTATGGTATTGCGATGGGTCTGGC-3'
	Reverse	5'-ACCTTTCTTCTCAATGATTTGATACGCCGC-3'

Underlines indicate mutation sites.

instructions. The sequences of the polymerase chain reaction primers used are listed in Table 1.

Enzyme expression and purification

WT and mutant enzymes were expressed and purified as described previously¹⁴. Each expression plasmid was transformed into *Escherichia coli* BL21(DE3). Recombinant cells were cultured in Luria–Bertani medium with 30 µg/mL kanamycin at 37°C and shaken at 200 r/min for 1 h. Expression of the recombinant protein was induced by adding 100 µmol/L isopropyl β-D-thiogalactopyranoside to the Luria–Bertani medium at 37°C for 19 h. The cells were collected by centrifugation and resuspended in buffer A (20 mmol/L potassium phosphate, pH 7.5). After sonication on ice, the cell extracts were centrifuged and the supernatants were collected. The protein solution was applied to a His GraviTrap™ Ni-chelating affinity chromatography column (Cytiva, Uppsala, Sweden) equilibrated with buffer A containing 500 mmol/L NaCl and 20 mmol/L imidazole. The bound protein was eluted stepwise using buffer A containing 500 mmol/L NaCl and 100–500 mmol/L imidazole. The protein solution was dialyzed against buffer A to remove NaCl and imidazole.

Finally, the homogeneity of each purified enzyme was verified by sodium dodecyl sulfate-polyacrylamide gel electrophoresis (SDS–PAGE). The molecular weight was determined by SDS–PAGE, and the protein concentration was quantified using the Bradford assay (Takara Bio Inc., Shiga, Japan).

Dehydrogenase activity assay

The LDH reaction is reversible, and substrate reduction proceeds simultaneously with oxidation of

the coenzyme NADH. The PYR, 2OBA, and PPY dehydrogenase activities of the WT and mutant enzymes were monitored based on the decrease in NADH concentration as described previously¹⁴. The time-dependent spectral change at 340 nm was measured against a blank to quantify NADH consumption using the molar extinction coefficient (6300 L·mol⁻¹·cm⁻¹). The enzyme solution (0.05 mL) was added to the assay solution (1.0 mL) containing 0.1 mol/L potassium phosphate buffer (pH 6.0), 10 mmol/L substrate [either sodium PYR (Nacalai Tesque, Inc.), sodium 2OBA (Tokyo Chemical Industry Co., Ltd., Tokyo, Japan), or sodium PPY (Sigma-Aldrich, St. Louis, USA)], 10 mmol/L D-fructose-1,6-bisphosphate, and 0.2 mmol/L NADH. One unit of activity was defined as the amount of enzyme that reduces 1 µmol of NADH per minute at 30°C. All data were averaged over three independent experiments.

2OBA assay

The decrease in NADH absorbance was measured at 340 nm using a spectrophotometer (U-3900; Hitachi, Tokyo, Japan). The working solution contained 0.1 mol/L potassium phosphate buffer (pH 6.0), 12 U/mL mutant enzyme, 10 mmol/L D-fructose-1,6-bisphosphate, and 0.2 mmol/L NADH. Subsequently, 900 µL of working solution was preheated at 30°C for 2 min, and 30 µL of 2OBA (0–2.0 mmol/L) was added. The changes in absorbance at 340 nm were measured in real time at 30°C for 5 min. The dilution linearity was calculated from the absorbance at 5 min. All data were averaged over three independent experiments.

3. Results and discussion

Mutation design of gs-LDH for high 2OBA affinity and 2OBA dehydrogenase activity

The dehydrogenase activity of gs-LDH toward 2OBA was approximately 57% that of PYR (Table 2). Because 2OBA is lightly bulkier than PYR owing to its methyl group (Fig. 1), an *in silico* mutation design for slightly expanding the substrate-binding site of gs-LDH was used to develop a 2OBA-specific dehydrogenase.

The structure of gs-LDH–2OBA complex was constructed by docking simulation (Fig. 2), resulting in the identification of the Q-to-V mutation at

position 102, which considered the substrate-binding site in accordance with the 2OBA structure and its interactions with the methyl group. This mutation expanded the substrate-binding pocket on the methyl side of 2OBA and enhanced its hydrophobicity around the methyl group (Fig. 2). The Q102V mutant was predicted to be more energetically stable in binding with 2OBA than the WT and was selected as a candidate for improving 2OBA specificity.

The expression plasmid for the Q102V mutant was generated using site-directed mutagenesis. Subsequently, the WT and mutant gs-LDHs were purified to homogeneity from the recombinant *E. coli* strains, as described in Materials and Methods. The molecular weight of all the enzymes was

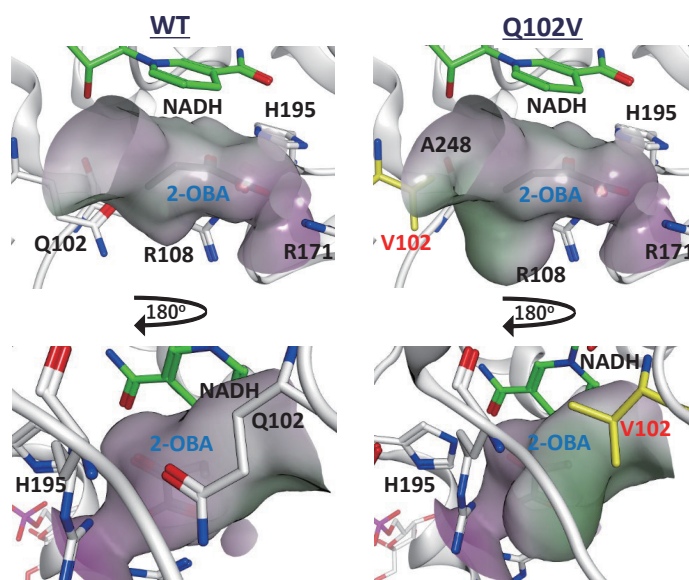


Fig. 2. Predicted complex structures of the wild-type (WT) and mutant with 2-oxobutyrate (2OBA). The main chain is represented by a ribbon model. The side chains, coenzyme NADH, and substrate 2OBA are represented using a stick model. The mutated residue (V102), NADH, 2OBA, oxygen, and nitrogen atoms are shown in yellow, green, gray, red, and blue, respectively. Substrate-binding pockets are indicated by transparent areas. Hydrophobic and hydrophilic regions of the substrate-binding surface are indicated in green and purple, respectively. H195 is a catalytic residue.

Table 2 Specific activities of WT and mutants

Enzyme	Specific Activity (U/mg)			2OBA/PYR (%)	2OBA/PPY (%)
	PYR	2OBA	PPY		
WT	561	319	236	56.9	135
Q102V	366	270	116	73.8	233
Q102V+A248L	43.3	268	118	619	226

2OBA/PYR and 2OBA/PPY represent 2OBA/PYR-specific activity ratio and 2OBA/PPY-specific activity ratio, respectively. Coefficient of variation for activity was less than 1.5%.

estimated to be approximately 37 kDa by SDS-PAGE, corresponding to the amino acid sequences (data not shown).

The enzymatic activities of the mutant were measured and compared with those of the WT (Table 2). The specific activity of Q102V against 2OBA was approximately 85% of that of the WT. The 2OBA/PYR-specific activity ratio for Q102V was 1.3-fold higher than that of the WT. Thus, the 2OBA specificity of the mutant improved although its specific activity decreased. Moreover, the 2OBA/PPY-specific activity ratio for Q102V was also 1.7-fold higher than that of the WT (Table 2).

However, the improvement in 2OBA specificity of Q102V was insufficient. The PYR dehydrogenase activity of Q102V remained high (approximately 65% of that of the WT) and was approximately 1.4-fold higher than its 2OBA dehydrogenase activity (Table 2). Further improvement in 2OBA specificity is desirable for its use as an analytical enzyme.

Additional mutation design to achieve high 2OBA affinity

Additional mutations combined with the Q102V mutation were investigated to improve 2OBA specificity. The enzyme-PYR complex structures were constructed by docking simulation, and double mutants with lower docking scores (S values) against PYR than those of Q102V were identified. Consequently, the additional A-to-L mutation at position 248 destabilized PYR binding. The S value represents the energetic stability of enzyme-substrate interactions; therefore, smaller values indicate more stable interactions, that is, high affinities. The S value for the Q102V-PYR complex was -5.6 , whereas that for the Q102V+A248L-PYR complex was -5.0 (Fig. 3). Therefore, the Q102V+A248L double mutant was predicted to bind PYR less stably than Q102V.

Furthermore, the 2D-depict close-up model of Q102V+A248L clearly showed spatial expansion of the substrate pocket (approximately 1.4-fold) and reduced interaction with PYR compared with that of

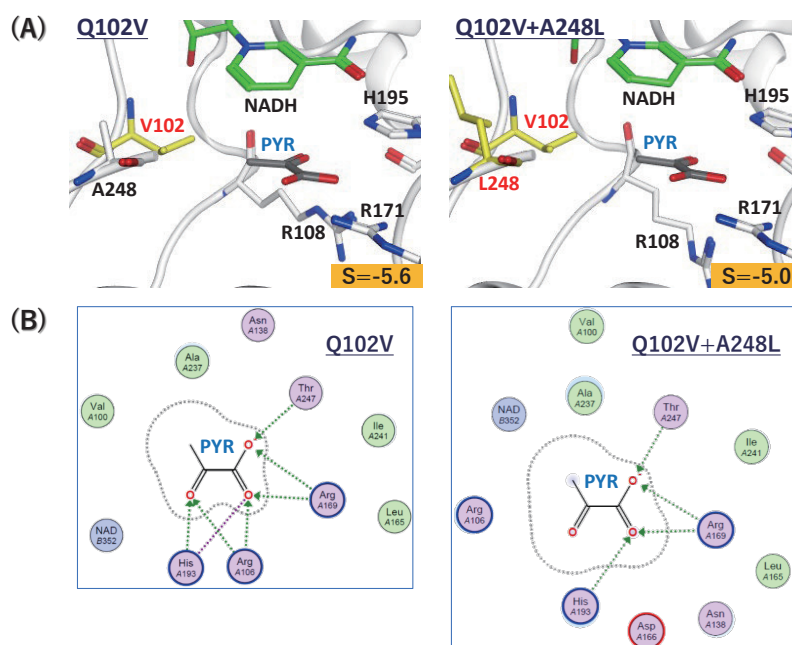


Fig. 3. Predicted complex structures of Q102V and Q102V+A248L with pyruvate (PYR). (A) The main chain is represented by a ribbon model. The side chains, coenzyme NADH, and substrate PYR are represented using a stick model. Mutated residues (V102 and L248), NADH, PYR, oxygen, and nitrogen atoms are shown in yellow, green, gray, red, and blue, respectively. The S value in each lower-right corner is the docking score, which indicates the energetic stability of the complex structure. (B) The 2D-depict close-up models around the substrate-binding sites. The substrate-binding area is indicated by the gray dotted curve. Hydrogen and ionic bonds are indicated by green dotted arrows and purple dotted line, respectively.

Q102V (Fig. 3). Specifically, the number of hydrogen and ionic bonds decreased from seven to four and their total energies increased from -40.6 kcal/mol to -30.3 kcal/mol. Thus, this mutation was identified as a candidate for further improvement in 2OBA specificity.

Properties of the double mutant

The gene encoding the double mutant Q102V+A248L was generated, and the enzyme was purified to homogeneity, as described in Materials and Methods. Enzymatic activities were compared between the WT, Q102V, and Q102V+A248L gs-LDHs (Table 2). Q102V+A248L exhibited high 2OBA specificity. Its PYR dehydrogenase activity was approximately 7.72% of that of the WT, and its 2OBA/PYR specific activity ratio was approximately 619% (11-fold higher) relative to that of the WT. Therefore, we developed a 2OBA-specific dehydrogenase.

2OBA assay using a double mutant

An endpoint assay reagent containing the 2OBA-specific double mutant was prepared and used in the 2OBA assay as described in the Materials and Methods section. The time courses of 2OBA measurement showed that endpoints were not completely attained within 5 min at most

concentrations tested (0.20–2.0 mmol/L) (Fig. 4A). In addition, high linearity of 5 min endpoint measurements was observed, with a correlation coefficient of 0.9976 in the range of 0 to 1.4 mmol/L 2OBA (Fig. 4B). These results suggest that the Q102V+A248L double mutant can be used for endpoint assays of 2OBA within the range measured in this study. Application to actual samples will be important for future practical use.

4. Conclusion

As a new subject of rational design, a 2OBA-specific dehydrogenase was developed through structure-based enzyme design of gs-LDH. The only structural difference between 2OBA and the native substrate PYR is the presence of a methyl group (Fig. 1). Because the 2OBA specificity of Q102V, which was identified in terms of spatial expansion and enhanced hydrophobicity by *in silico* analysis (Fig. 2), was insufficient, the additional mutation A248L, for which energetic destabilization of PYR binding was revealed by docking analysis (Fig. 3), was introduced. The 2OBA/PYR activity ratio of the double mutant was significantly improved; thus, a 2OBA-specific dehydrogenase was successfully developed (Table 2). An endpoint assay using a reagent containing the double mutant

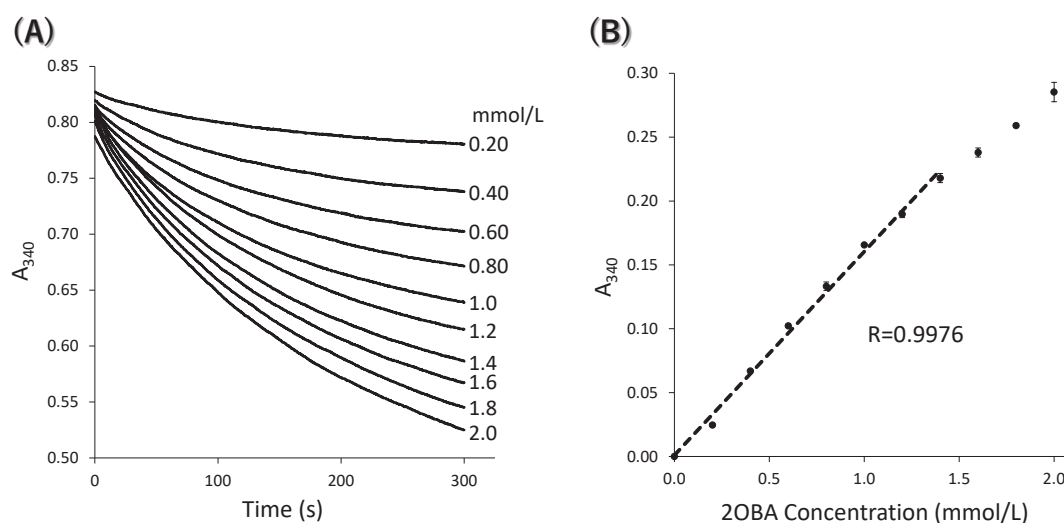


Fig. 4. 2-oxobutyrate (2OBA) assay using Q102V+A248L. (A) Reaction time course. The 2OBA concentrations are shown in the graph. (B) Linearity. Error bars represent standard deviation ($n = 3$). R values represent the correlation coefficients.

preliminarily confirmed the practicality of 2OBA quantification (Fig. 4).

This is the first study to report the development of a 2OBA-specific enzyme based on rational mutation design of LDH. Although it is difficult to alter the specificity of highly similar substrates, this study serves as a successful model case, suggesting in the importance of rational mutation design for the development of analytical enzymes. Furthermore, LDH can be used to develop other analytical enzymes. Because LDH does not require a follow-up enzyme, the developed enzymes are expected to simplify measurements.

Conflicts of interest

The authors declare no conflict of interest.

Acknowledgements

We thank Shotaro Yamaguchi for technical support. We are grateful to Dr. Yuya Shimozawa for helpful discussion. We would like to thank Editage (www.editage.jp) for the English language editing.

References

1. Wigley DB, Gamblin SJ, Turkenburg JP, Dodson EJ, Piontek K, Muirhead H, and Holbrook JJ: Structure of a ternary complex of an allosteric lactate dehydrogenase from *Bacillus stearothermophilus* at 2.5 Å resolution. *J Mol Biol*, 223:317-335, 1992.
2. Wilks HM, Hart KW, Feeney R, Dunn CR, Muirhead H, Chia WN, Barstow DA, Atkinson T, Clarke AR, and Holbrook JJ: A specific, highly active malate dehydrogenase by redesign of a lactate dehydrogenase framework. *Science*, 242:1541-1544, 1988.
3. Shimozawa Y and Nishiya Y: Malate dehydrogenase of *Geobacillus stearothermophilus*: A practically feasible enzyme for clinical and food analysis. *Int J Anal Bio-Sci*, 7:59-67, 2019.
4. Shimozawa Y, Himiyama T, Nakamura T, and Nishiya Y: Structural analysis of diagnostic enzymes: Differences in substrate specificity between malate dehydrogenase and lactate dehydrogenase [Jpn]. *J Anal Bio-Sci*, 44:151-159, 2021.
5. Shimozawa Y, Himiyama T, Nakamura T, and Nishiya Y: Structural analysis and reaction mechanism of malate dehydrogenase from *Geobacillus stearothermophilus*. *J Biochem*, 170:97-105, 2021.
6. Shimozawa Y, Himiyama T, Nakamura T, and Nishiya Y: Increasing loop flexibility affords low-temperature adaptation of a moderate thermophilic malate dehydrogenase from *Geobacillus stearothermophilus*. *Protein Eng Des Sel*, 34:gzab026, 2021.
7. Shimozawa Y, Mtsuhisa H, Nakamura T, Himiyama T, and Nishiya Y: Reducing substrate inhibition of malate dehydrogenase from *Geobacillus stearothermophilus* by C-terminal truncation. *Protein Eng Des Sel*, 35:gzac008, 2022.
8. Davies DD and Davies S: Purification and properties of L(+)-lactate dehydrogenase from potato tubers. *Biochem J*, 129:831-839, 1972.
9. Steinbüchel A and Schlegel HG: NAD-linked L(+)-lactate dehydrogenase from the strict aerobic *Alcaligenes eutrophus* 1. purification and properties. *Eur J Biochem*, 130:321-328, 1983.
10. Binay B, Sessions RB, and Karagüler NG: A double mutant of highly purified *Geobacillus stearothermophilus* lactate dehydrogenase recognises L-mandelic acid as a substrate. *Enzyme Microb Technol*, 52:393-399, 2013.
11. Li JF, Li XQ, Liu Y, Yuan FJ, Zhang T, Wu MC, and Zhang JR: Directed modification of L-LcLDH1, an L-lactate dehydrogenase from *Lactobacillus casei*, to improve its specific activity and catalytic efficiency towards phenylpyruvic acid. *J Biotechnol*, 281:193-198, 2018.
12. Wu A, Bai Y, Fan TP, Zheng X, and Cai Y: Modified catalytic performance of *Lactobacillus fermentum* L-lactate dehydrogenase by rational design. *Syst Microbiol Biomanuf*, 2:473-486, 2022.
13. Hiruta M and Nishiya Y: Creation of an L-mandelate oxidase via structure-guided design of engineered lactate oxidase. *Int J Anal Bio-Sci*, 6:25-29, 2018.
14. Nakamura M and Nishiya Y: Development of a phenylpyruvate-specific dehydrogenase through structure-based enzyme designs and its application in a phenylpyruvate assay. *Int J Anal Bio-Sci*, 13:16-23, 2025.
15. Kumar T, Sharma GS, and Singh LR: Homocystinuria: therapeutic approach. *Clin Chim Acta*, 458:55-62, 2016.
16. Gerrard A and Dawson C: Homocystinuria diagnosis and management: it is not all classical. *J Clin Pathol*, 75:744-750, 2022.
17. Nishiya Y, Toyama F, and Zhang Y: Computational

insights for coenzyme interactions in wild-type and mutant sarcosine oxidases. *Int J Anal Bio-Sci*, 11:111-116, 2023.

18. Nishiya Y, Ishihara H, Zhang Y, and Toyama F:

Rational alteration of the pH profile of sarcosine oxidase by site-directed mutagenesis around the active site. *Int J Anal Bio-Sci*, 12:15-20, 2024.